

Craze growth and fracture in ABS polymers

L. V. NEWMANN*, J. G. WILLIAMS

Department of Mechanical Engineering, Imperial College of Science and Technology, London, UK

Craze growth and fracture tests have been conducted on two grades of ABS. Crazeing is shown to be governed by a relaxation process which may be accounted for using a modified Dugdale model. The results of the fracture tests indicate that there are two values of toughness appropriate to a complete description of the failure process over a wide range of temperatures. The first of these occurs at the initiation of cracking and is shown to be a geometry-independent parameter, whilst the second, which takes place at maximum load, is dependent on the loading mode employed.

1. Introduction

A significant advance in the understanding of the fracture behaviour of engineering materials has been afforded by the practical utilization of the theories of linear elastic fracture mechanics (LEFM). In particular, it has become possible to obtain a quantitative measure of toughness, free from the influence of specimen geometry, a most valuable asset in accurate material assessment. Since the fundamental theory of LEFM is based on the assumption of brittle failure involving negligible plasticity at the crack tip, it is a good model for the behaviour of polymeric materials, such as poly(methyl methacrylate) and polystyrene. The enhanced toughness of rubber-modified materials, such as high-impact polystyrene (HIPS) and acrylonitrile-butadiene-styrene (ABS), however, is a direct result of their capacity to form large areas of dense crazeing and so the applicability of the theory in toughness prediction for them still remains to be demonstrated.

Recent work on impact polystyrene by Ferguson *et al.* [1] and Nikpur and Williams [2] has shown that, provided adequately large samples are tested, either a critical stress intensity or constant crack opening displacement (COD) criterion can be used to describe failure. The occurrence, however, of slow crack growth prior to the attainment of maximum toughness has led to the need to define two separate K values, the

first appropriate to the initiation of cracking and the second to maximum load. Nikpur and Williams have further identified a plane strain toughness, K_{C1} , as being that appropriate to failure of the base polymer matrix, measured K values being necessarily higher than this due to the occurrence of crazeing.

Specific studies on the toughness of ABS have been confined largely to impact testing [3, 4], although high-speed tensile [5] and puncture tests [6] are also reported in the open literature. This paper describes both craze growth and fracture tests carried out on two grades of ABS, the approach used being similar to that adopted by Nikpur and Williams, and Ferguson *et al.* A model of relaxation-controlled crazeing based on the assumption of a constant COD is shown to describe the experimentally determined craze growth results well. An unmodified critical stress intensity criterion has been found to be appropriate for the evaluation of toughness at crack initiation, K_{init} , whilst incorporation of a crack-length correction allows its extension to cover the case of maximum load. Both toughness values have been measured over the temperature range +20 to -100°C for each of the two test materials.

2. Fracture mechanics theory

Both the fundamental LEFM theory for brittle materials and the Dugdale model, which accounts

*Present address: Ove Arup and Partners, 13 Fitzroy Street, London, UK.

for a line plastic zone at the crack tip, have been well documented elsewhere, but a brief summary of each will be given here.

Griffith [7] proposed that fracture in a perfectly brittle material would occur when the energy released by the infinitesimal extension of a pre-existing flaw was greater than that absorbed in the necessary increase in surface area. This idea was later found to be applicable to the more practical case of a material whose predominant energy absorption mechanism at the crack tip involves highly localized plastic deformation. In either case, a criterion for failure may be expressed in terms of a critical value of strain energy release rate G , G_C . Irwin [8] has further shown that G is equivalent to the stress intensity factor, K , at the crack tip, a parameter dependent only on loading and sample geometry, the relation being:

$$G = \eta \frac{K^2}{E}$$

where E is Young's modulus, and $\eta = 1 - \nu^2$ (plane strain) or $\eta = 1$ (plane stress).

Failure, may, therefore, also be characterized by a critical K , K_C , and the expression relating this to the critical stress at fracture, σ_C , in a finite sample of given geometry is:

$$K_C^2 = \sigma_C^2 Y^2 a \quad (1)$$

where a is the length of the flaw under consideration, and Y is a correction factor dependent on the specific specimen geometry. In practice, if the theory is valid for a particular material, the value of K_C predicted by experiment should be independent of both the length of the flaw and the configuration of specimen used for testing. In this event, K_C may be considered to be a material property at the particular temperature and strain rate used.

Although it has been stated that the theory accounts for limited plastic deformation at the crack tip, the extent to which this is permissible is still limited, so that, in many practical cases, it is necessary to incorporate a further correction factor. To a first approximation, the local stress relaxing influence of the plastic zone can be accounted for by using a crack-length correction of magnitude r_p , where:

$$r_p = \frac{1}{2\pi} \frac{K^2}{\sigma_y^2}$$

σ_y being the yield stress of the material under consideration.

A further more significant modification of the linear elastic theory devised to take into account the effects of crack tip yielding is afforded by the Dugdale model [9], which incorporates a line plastic zone at the tip of the crack. By assuming that no stress singularity exists at the tip of the yield zone, the length of the latter can be shown to be given by:

$$\Delta = \frac{\pi \sigma^2 \pi a}{8 \sigma_y^2} = \frac{\pi K^2}{8 \sigma_y^2}, \quad (2)$$

where σ is the remote applied stress, and a is the crack half-length in an infinite plate.

A lateral opening of the crack tip assumed implicitly in the Dugdale model was noted to occur in practice in laboratory specimens. This quantity is known as the crack opening displacement (COD) and may be expressed for low values of remote stress applied to an infinite plate as:

$$\delta = \frac{\sigma^2 \pi a}{E \sigma_y} \quad (\text{plane stress}).$$

Dugdale model solutions have also been evaluated for practical test geometries using a finite element technique [10]. In these, the COD is usually expressed in non-dimensional form as:

$$\delta^* = \frac{\pi E \delta}{4 \sigma_y D \eta},$$

D being a characteristic length associated with the specimen of interest. The value of the concept of COD lies in the possibility of utilizing it as a characterization parameter, reflecting the state of the crack tip strain, so that once more failure can be identified with a critical value of that parameter.

Williams and Marshall [11] have shown that the Dugdale model can be modified to predict relaxation controlled craze growth. Recognizing that the state of the relaxation varies along the length of the craze, and assuming the stress at any point to decay with the time according to the relation:

$$\sigma_{cr} = \sigma_0 t^{-n}$$

where σ_0 is the unit time craze stress, and n is a constant, they define an average craze stress as:

$$\bar{\sigma}_{cr} = \frac{1}{t} \int_0^t \sigma_{cr} dt$$

so that:

$$\bar{\sigma}_{cr} = \frac{\sigma_0 t^{-n}}{1-n}$$

This, taken together with Equation 2 from the Dugdale model, gives:

$$\Delta = \frac{\pi K^2}{8 \sigma_0^2} (1-n)^2 t^{2n} \quad (3)$$

3. Experimental work

Two grades of ABS were tested during the course of this experimental programme. The first was a commercially available material (ASTM properties: tensile modulus = 2160 MN m⁻², tensile yield strength = 41 MN m⁻², Izod impact strength = 294 J m⁻¹), denoted here as ABS-1. ABS-2 had a slightly higher elastomer content, and different strength characteristics (tensile yield strength = 22.5 MN m⁻², tensile modulus = 1420 MN m⁻²).

Two thicknesses of ABS-1 were available for testing, nominally 5 mm and 13 mm, the former being extruded, and the latter compression moulded. ABS-2 was compression moulded to 5 mm thickness.

In view of the need to generate reproducible sharp notches in all samples to satisfy the requirements of adopting a fracture mechanics approach, the notching technique used was as follows. Rough notches were cut initially to within 0.5 mm of the final depth required using a band saw or 60° milling cutter. These were then taken down to size with a 20° flycutter hand sharpened to as fine a point as possible.

3.1. Craze growth testing

The study of craze growth under the action of a constant applied load was conducted using single edge notch (SEN) specimens of ABS-1 having nominal dimensions 50 mm × 150 mm. Samples of crack lengths 2, 8, 10 and 12 mm were tested under various loads using a simple lever arm rig in order to generate a range of applied stress intensities. Care was taken to keep the loads below a level sufficient to cause the cracks to advance. Measurements of the overall craze length were made as a function of time elapsed beyond loading using a travelling microscope. Care was taken that the illumination of the specimen did not give rise to any significant localized heating effect.

3.2. Fracture testing

All the fracture testing conducted was organized

TABLE I

Material	Material thickness	
	5 mm	13 mm
ABS-1	SEN-S 3PB	SEN-S SEN-L
ABS-2	SEN-S	—

SEN-S = single edge notch, 50 mm × 150 mm.

SEN-L = single edge notch, 150 mm × 300 mm.

3PB = three-point bend, 150 mm × 20 mm.

into batches of specimens having a range of crack lengths. Details of the materials and geometric configurations used are given in Table I.

Utilization of specimens of differing overall dimensions was made to afford evidence of any significant size effects prevailing. Tests were conducted on an Instron Universal Testing Machine at a fixed cross-head rate of 0.2 cm min⁻¹.

The first set of data was obtained at room temperature (+20°C ± 1°C, 50% ± 5% R.H.), subsequent series being conducted at 20°C intervals down as far as -100°C. Low-temperature conditions were achieved by regulating the flow of vapourized liquid nitrogen through an insulated chamber surrounding the specimen. With sufficient care, it was possible to maintain the temperature to within one or two degrees of that required. Each specimen was allowed to normalize in the chamber for at least 15 min prior to testing to allow thorough cooling to take place.

Continuous observation of the specimen through a travelling microscope allowed the onset of cracking to be recorded on the Instron chart with a remote event marker. Additionally, by adhering a small grid to the side of the specimen ahead of the crack tip, it was possible to monitor the progress of the crack as a function of applied load, in the same way.

4. Results

4.1. Craze growth experiments

Observation of the crack tip region on application of load showed a fine line-like craze bundle, similar to the form of that assumed in the Dugdale model, to develop and extend slowly with time. Equation 3 indicates that, if the model is valid, craze length plotted on a log scale as a function of time should be linear of slope 2n. Fig. 1 shows such a plot for several specimens, supporting this relation and predicting a value of n of 0.04 which,

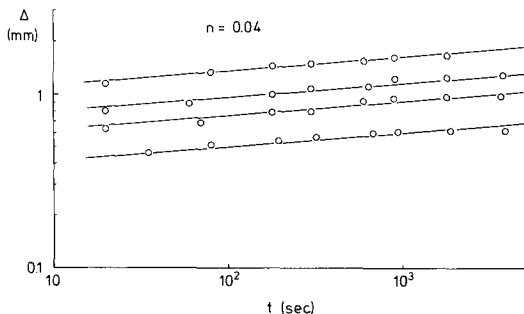


Figure 1 Craze length plotted as a function of time: nominal stress intensity = $1.7 \text{ MN m}^{-3/2}$.

being low, indicates the material to have only a very slight time dependence. Further confirmation of the validity of the model is afforded by plotting the craze length against the square of the applied stress intensity, at a fixed elapsed time, t_1 , as shown in Fig. 2. Results for all four initial crack lengths fall on the same line, and the consistency of the data is excellent. The value of unit time craze stress, σ_0 , indicated from the slope of the plot is 44.9 MN m^{-2} , very close to the measured yield stress of the material.

4.2. Fracture testing

A similar pattern of behaviour was observed in all specimens tested at temperatures down to -80°C . The early stages of deformation were fully elastic, as reflected by the linear load–deflection record.

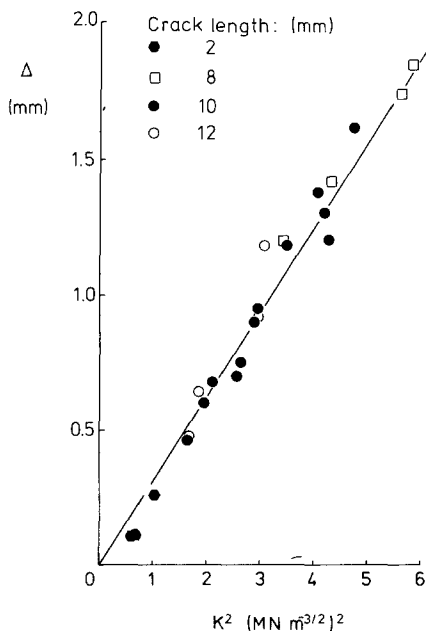


Figure 2 Dependence of craze length on the square of applied stress intensity at time $t = 10^3$ sec.

As loading continued, examination of the crack-tip region showed the development of a small line-like craze-whitened bundle which accompanied a gradual blunting of the crack tip. Slow, steady, forward motion of both the crack and craze fronts was accompanied by an increased curvature of the load–deflection record until, eventually, the latter reached a maximum. In some cases, the crack accelerated rapidly and ran through the remainder of the specimen, whilst in others it accelerated for a short distance but arrested before reaching the back face. In contrast to this, specimens tested at -100°C showed no craze whitening, and failed in a completely unstable, brittle manner, producing a triangular load–deflection trace.

It is clear from these observations that, with the exception of very low temperature fractures, it is possible to identify two significant events occurring in the course of a typical fracture – crack initiation and maximum load, each of which will be discussed in the following section.

5. Room temperature tests

5.1. Crack initiation

In order to assess whether there exists a characteristic toughness associated with the initiation of cracking, the results of all the tests conducted were plotted according to Equation 1 as $\sigma^2 Y^2$ against $1/a$ using the marked initial load and initial value of crack length, a_0 . Fig. 3 shows the results

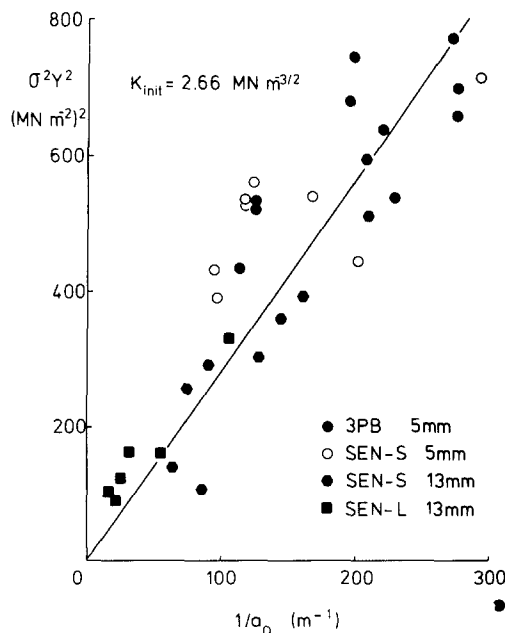


Figure 3 Crack initiation data: ABS-1.

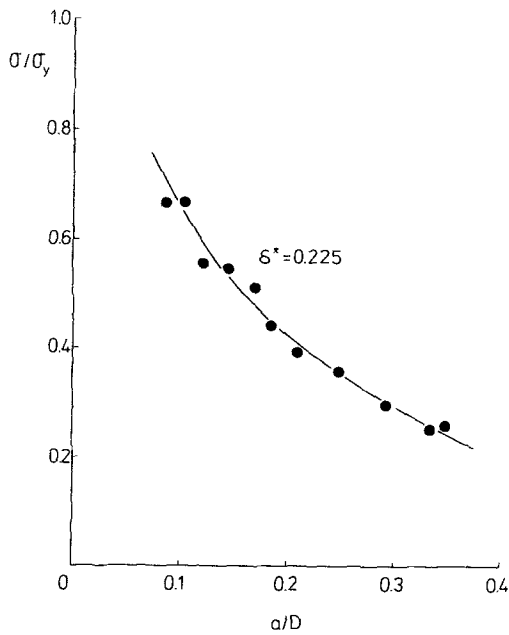


Figure 4 Crack initiation data plotted according to the Dugdale model: ABS-2.

obtained in this way from each of the four test series conducted. Not only are the data within each batch well represented by the theory, but the different specimen configurations are self-consistent, indicating K_{init} to be a truly geometry-independent parameter.

Confirmation of the validity of this toughness model for application to crack initiation is afforded by comparing the experimental results with those predicted by assuming a constant COD at failure. Fig. 4 shows data from samples of ABS-2. The curve drawn through the points represents a constant COD of 0.18mm which predicts an equivalent value of K_{init} of $2.30 \text{ MN m}^{-3/2}$, which compares excellently with $2.06 \text{ MN m}^{-3/2}$ measured directly (Fig. 5).

5.2. Maximum load data

Use of the straightforward LEFM equation is inadequate for description of the maximum load condition. This is illustrated by Fig. 6 where toughness apparently falls off as the crack length is reduced. Such an effect is not surprising since no account has been taken of the slow crack growth preceding attainment of maximum toughness. Fig. 7 shows the relation between crack length at maximum load, a_{max} , and initial crack length, a_0 , for SEN specimens of ABS-1 at room temperature, which suggests that the extent of slow growth is constant. If, now, a crack length

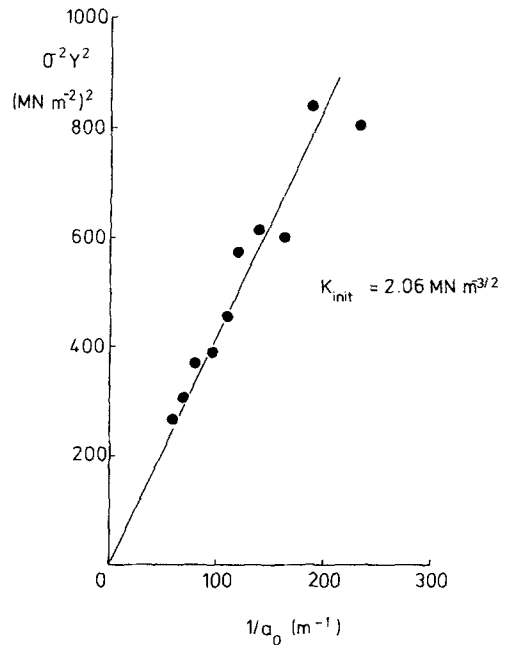


Figure 5 Crack initiation data: ABS-2.

correction, a^* , equal to this measured value is applied to each specimen, the apparent toughness, $K_{IC_{app}}$, measured becomes independent of geometry within any given batch of specimens, an effect which can be explained as follows (Fig. 8). By increasing the crack length, allowance is made for the rise in specimen compliance effective during slow growth. Since the extent of this

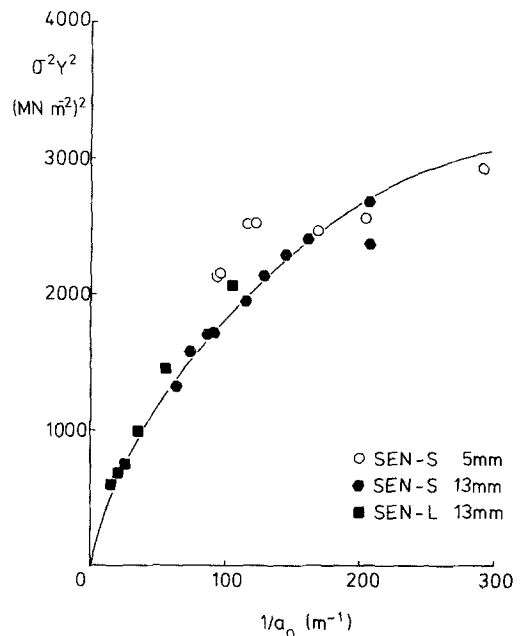


Figure 6 Maximum load data, uncorrected: ABS-1.

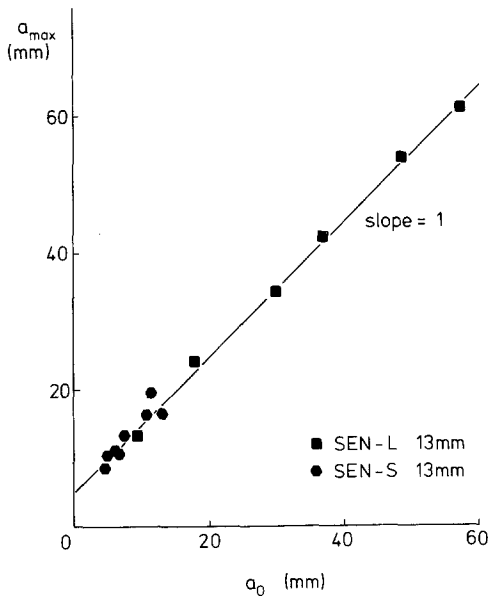


Figure 7 Crack length at maximum load plotted as a function of initial crack length: ABS-1.

rise becomes increasingly pronounced as the crack length is reduced, the correction procedure will tend to compensate more for shorter crack lengths, thus restoring the data to linearity.

A more detailed examination of the results from the different batches of specimens of ABS-1 tested shows that all three types of SEN sample

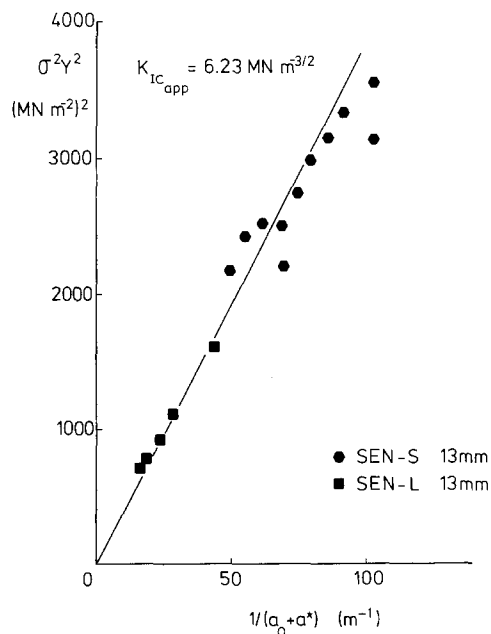


Figure 8 Maximum load data incorporating crack length correction: ABS-1.

predict a similar toughness value, so that there is evidently neither size nor thickness effect operative. In contrast to this, however, the toughness predicted by the three-point bend samples is significantly lower than that in tension. It seems, therefore, that, whilst the toughness of initiation, K_{init} , is truly geometry-independent, the maximum toughness attainable is not, and is therefore not a material property.

The difference between the toughness predicted by three-point bend and SEN specimens at maximum load may be explained in terms of there being a difference in the degree of constraint applied to the crack tip. In the case of three-point bend, the crack is forced to run towards a region of compressive stress, resulting in a reduction in the extent of slow crack growth prior to maximum load (0.8 mm as compared with 4.8 mm in SEN for ABS-1). Theoretically, then, with sufficient constraint, ductility could be suppressed to such an extent that no slow growth would take place at all, and the maximum load would then occur at crack initiation. By this argument, K_{init} can be seen as the minimum toughness value likely to be displayed in any fracture event in ABS under normal conditions (i.e. excluding adverse effects of environment, etc.), whilst, under most circumstances, greater values will be attained.

6. Low temperature testing

6.1. Crack initiation

As outlined earlier, no significant change was brought about in the pattern of fracture behaviour by a reduction in the test temperature until a level of -100°C was reached. At this point, crack initiation and maximum load were coincident and the specimens completely devoid of craze whitening. A value of fracture toughness of $2.10\text{ MN m}^{-3/2}$ was measured for ABS-1, this being some 20% lower than that at $+20^{\circ}\text{C}$. This loss in ductility and toughness is directly attributable to the fact that, at temperatures below about -85°C , the elastomeric phase is no longer effective in generating crazes due to being below its glass transition temperature.

Between $+20$ and -80°C , K_{init} is found to rise gradually, reaching a peak in the region of the glass transition temperature (Fig. 9). The increase in measured toughness coincides with a gradual change in the appearance of the yield zone ahead of the crack tip, the visible whitening becomes less like a bundle of individual crazes

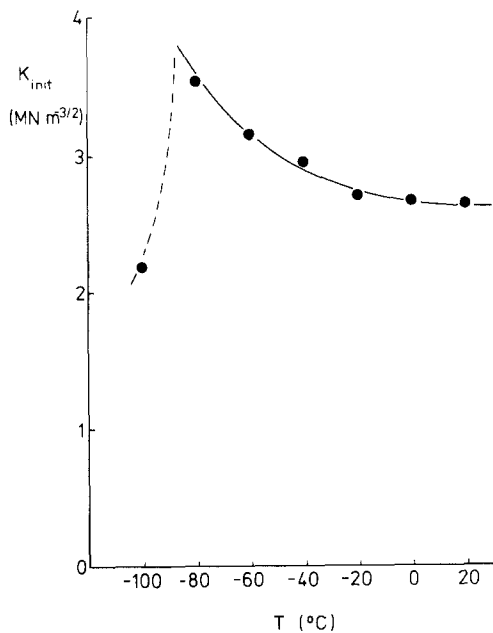


Figure 9 Dependence of initiation toughness on temperature: ABS-1.

and more a homogeneous cloudiness. It is possible that this may represent a transition from crazing to shear banding as the predominant mechanism of plastic deformation.

Once again, the total geometric independence of K_{init} observed at room temperature was apparent throughout the low-temperature region, SEN and three-point bend specimens yielding the same results.

6.2. Maximum load

All the maximum load data collected at low temperatures were analysed exactly as described for the room temperature results. This again involved the measurement of slow growth for each specimen, a procedure which revealed a surprising result. Since the specimens tested at -100°C were found to be completely brittle, it was anticipated that the extent of slow growth would drop gradually to zero as the test temperature approached this value. In practice, however, the opposite trend was recorded, as shown for ABS-2 in Fig. 10. Such a monotonic increase was not apparent with the maximum load, which was found to rise gradually until a temperature of -40°C was reached, and then to drop again. This is reflected in the final values of toughness calculated, as shown in Figs. 11 and 12.

The discrepancy between $K_{IC_{app}}$ evaluated in

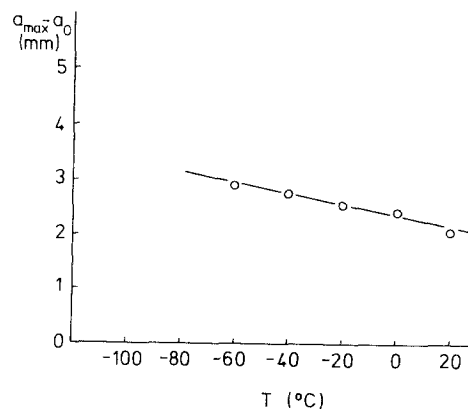


Figure 10 Slow growth plotted as a function of temperature: ABS-2.

tension and bending remains over most of the temperature range investigated, the two values only being coincident at -100°C where the apparent toughness and initiation toughness are equivalent anyway. This observation lends further weight to the proposal that it is the presence of the large plastic zone and the extent to which it is constrained in different geometric configurations which give rise to the discrepancy in the apparent toughness measured.

7. Discussion

The outcome of the tests described in this paper suggests that the value of fracture toughness, K_{init} ,

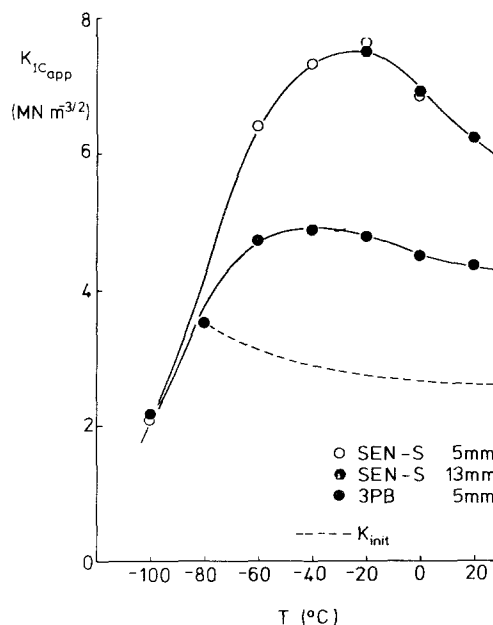


Figure 11 Dependence of toughness at maximum load on temperature: ABS-1.

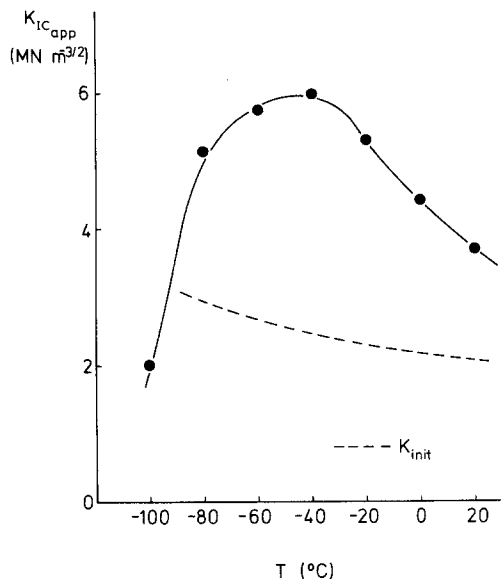


Figure 12 Dependence of toughness at maximum load on temperature: ABS-2.

pertaining to crack initiation is a fundamental material property, being quite independent of the geometry of specimen used to measure it. Beyond initiation, a further increase in toughness usually takes place, but the extent to which a rise occurs is dependent on the mode of loading employed.

At first, it seems reasonable to suppose that K_{init} might be equivalent to the toughness of the base matrix material of the polymer. However, since there is always a highly deformed region of whitened material in the immediate vicinity of the notch tip at crack initiation, the concept of the crack initiating within the matrix alone is unreasonable. Furthermore, the value of K_{init} measured at room temperature is greater than at -100°C which, since the elastomeric phase is below its glass transition point, must be representative of the matrix toughness. In general, toughness drops as the temperature rises, so that at room temperature the matrix toughness must be less than K_{init} .

It remains a possibility, then, that K_{init} is a composite quantity based on the matrix toughness plus a term accounting for craze generation or ductility. In this instance, however, there is no way of ascertaining what the relation between these quantities might be, since the absolute value of matrix toughness is unknown. Neither

is it possible to separate values appropriate to conditions of plane strain and plane stress, as done by Nikpur and Williams for HIPS, since the two material thicknesses tested gave identical results.

8. Conclusions

Craze growth in ABS is a relaxation controlled process, being well described by a modified Dugdale model due to Williams and Marshall [11]. The degree of time dependence exhibited is low, so that, under low constant loads, craze growth is slow.

Linear elastic fracture mechanics has been used to identify two characteristic toughnesses during a complete fracture event in ABS. The first of these occurs at crack initiation, K_{init} , and has been shown to be geometry independent and therefore a material property. The second toughness, occurring at maximum load, has been found to depend on the mode of loading (i.e. tension or bending) but is constant for different specimen geometries broken under the same mode.

Acknowledgement

The authors wish to thank Borg-Warner Chemicals for their generous financial support of this work.

References

1. R. J. FERGUSON, G. P. MARSHALL and J. G. WILLIAMS, *Polymer* **14** (1973) 451.
2. K. NIKPUR and J. G. WILLIAMS, *J. Mater. Sci.* **14** (1979) 467.
3. H. R. BROWN, *ibid* **8** (1973) 941.
4. L. V. NEWMANN and J. G. WILLIAMS, *Polymer Eng. Sci.* **18** (1978) 893.
5. P. J. FENELON, Proceedings of SPE 32nd ANTEC, San Francisco, California, 13–16 May (1974) p. 106.
6. V. E. MALPASS, *Appl. Polym. Symp.* **5** (1967) 87.
7. A. A. GRIFFITH, Proceedings of the 1st International Congress on Applied Mechanics, Delft, Holland (1924).
8. G. R. IRWIN, *J. Appl. Mech.* **24** (1957) 361.
9. D. S. DUGDALE, *J. Mech. Phys. Solids* **8** (1960) 100.
10. D. J. HAYES and I. G. WILLIAMS, *Int. J. Fract. Mech.* **8**(3) (1972) 239.
11. J. G. WILLIAMS and G. P. MARSHALL, *Proc. Roy. Soc. London* **A342** (1975) 55.

Received 26 July and accepted 13 September 1979.